

*Letter to the Editor***Evolution of the Galactic potential and halo streamers with future astrometric satellites**HongSheng Zhao<sup>1</sup>, Kathryn V. Johnston<sup>2</sup>, Lars Hernquist<sup>3</sup>, and David N. Spergel<sup>4</sup><sup>1</sup> Sterrewacht Leiden, Niels Bohrweg 2, 2333 CA, Leiden, The Netherlands<sup>2</sup> Institute for Advanced Study, Princeton, NJ 08450, USA<sup>3</sup> University of California, Board of Studies in Astronomy and Astrophysics, Santa Cruz, CA 95064<sup>4</sup> Princeton University, Princeton University Observatory, Princeton, NJ 08540, USA

Received 25 May 1999 / Accepted 12 July 1999

**Abstract.** ESA's Global Astrometric Interferometer for Astrophysics (GAIA) holds the promise of mapping out the detailed phase space structure of the Galactic halo by providing unprecedented annual proper motion and parallax of 1–10  $\mu\text{as}$  astrometric accuracy (Gilmore et al. 1998). Unlike NASA's Space Interferometry Mission (SIM), which will achieve similar accuracies but is a pointed instrument, GAIA will be able to construct a global catalogue of the halo. Here we study proper motions of giant branch stars in a tidal debris torn from a small satellite system in the halo. We follow the evolution of a cold stream on a polar orbit between 8–50 kpc in a variety of histories of the Galactic potential, and observe the bright ( $V < 18\text{mag}$ ) members of the debris tail with GAIA accuracy. We simulate effects due to the growing or flipping of the Galactic disk over the past 4 Gyrs or the perturbation from a massive accreted lump such as the progenitor of the Magellanic Clouds. Our simulations suggest that the results of Johnston, Zhao, Spergel & Hernquist (1999) and Helmi, Zhao & de Zeeuw (1999) for static Galactic potentials are likely to be largely generalizable to realistic time-dependent potentials: a tidal debris remains cold in spite of evolution and non-axial symmetry of the potential. GAIA proper motion measurements of debris stars might be used to probe both Galactic structure and Galactic history. We also study several other factors influencing our ability to identify streams, including accuracy of radial velocity and parallax data from GAIA, and contamination from random field stars. We conclude that nearby, cold streams could be detected with GAIA if these cousins of the Sagittarius stream exist.

**Key words:** Galaxy: evolution – Galaxy: formation – Galaxy: halo – Galaxy: kinematics and dynamics – Galaxy: structure – celestial mechanics, stellar dynamics

**1. Introduction**

Tidal streams in the Galactic halo are a natural prediction of hierarchical galaxy formation, where the Galaxy builds up its mass by accreting smaller infalling galaxies. They are often traced by luminous horizontal and giant branch (HB and GB) stars outside the tidal radius the satellite, by which we mean either a dwarf galaxy or a globular cluster in the Galactic potential. These extra-tidal stars have been seen for the Sagittarius dwarf galaxy (Ibata, Gilmore, & Irwin 1994) and for other dwarf galaxies and globular clusters (cf. Grillmair et al. 1998, Irwin & Hatzidimitriou 1995) as a result of tidal stripping, shocking or evaporation. That extra-tidal material (stars or gas clouds) traces the orbit of the satellite or globular cluster has long been known to be a powerful probe of the potential of the Galaxy in the halo, and has been exploited extensively particularly in the case of the Magellanic Clouds and Magellanic Stream and the Sagittarius dwarf galaxy.

Helmi, Zhao & de Zeeuw show that streams can be identified by as peaks in the distribution in the angular momentum space, measurable with GAIA. Once identified, we can fit a stream with an orbit or more accurately a simulated stream in a given potential. Johnston, Zhao, Spergel & Hernquist (1999) show that a few percent precision in the rotation curve, flattening and triaxiality of the halo is reachable by mapping out the proper motions (with SIM accuracy) and radial velocities along a tidal stream 20 kpc from the Sun. In particular, they show that the fairly large error in distance measurements to outer halo stars presents no serious problem since one can predict distances theoretically using the known narrow distribution of the angular momentum or energy along the tails associated with a particular Galactic satellite. We expect these results should largely hold for streams detectable by GAIA. These numerical simulations are very encouraging since they show that it is plausible to learn great deal about the Galactic potential with even a small sample of stream stars from GAIA. Some unaddressed issues include whether stream members will still be identifiable in angular momentum in potentials without axial symmetry, and

the robustness of both methods if the Galactic potential evolves in time.

Here we illustrate the effects of including a realistic evolution history of the Galaxy’s potential. The simulations are observed with GAIA accuracy. We discuss whether bright stars in a stream might still be identified using the 6D information from GAIA.

## 2. Streams in realistic time-varying potentials

### 2.1. Evolution of the Galactic potential

To simulate the effect of the evolution and flattening of the potential on a stream, we will consider a satellite orbiting in the following simple, flattened, singular isothermal potential  $\Phi(r, \theta, t)$

$$\Phi_G(r, \theta, t) = V_0^2 \left[ A_s \log r + \frac{\epsilon}{2} \cos 2\theta \right], \quad (1)$$

where

$$A_s(t) = 1 - \epsilon_0 + \epsilon(t), \quad \epsilon(t) = \epsilon_0 \cos \frac{2\pi t}{T_G}. \quad (2)$$

This model simulates the effect that the Galaxy becomes more massive and flattened in potential as it grows a disc. It is time-dependent but maintains a rigorously flat rotation curve at all radii, where  $(r, \theta)$  are the spherical coordinates describing the radius and the angle from the North Galactic Pole,  $t$  is defined such that  $t = 0$  would be the present epoch. The time-evolution is such that the Galactic potential grows from prolate at time  $t = -T_G/2$  to spherical at time  $t = -T_G/4$ , and then to oblate at  $t = 0$ ; a more general prescription of the temporal variation might include a full set of Fourier terms.

We adopt parameters

$$V_0 = 200 \text{ km s}^{-1}, \quad \epsilon_0 = 0.1, \quad (3)$$

for the present-day circular velocity, and the flattening of the equal potential contour of the Galaxy respectively. A small  $\epsilon_0$  guarantees a positive-definite volume density of the model everywhere at all time. We set  $T_G/4 = 4 \text{ Gyr}$ , a reasonable time scale for the growth of the Galactic disc.

We have also considered Galactic potentials with a flipping disc and with a massive perturber (Zhao et al. 1999). The results are qualitatively the same. In the following we will illustrate our points with the potential with a growing disc  $\Phi_G$ .

### 2.2. Evolution of the satellite

Following Helmi & White (1999), we assume that the particles in the disrupted satellite are initially distributed with an isotropic Gaussian density and velocity profile with dispersions  $0.4 \text{ kpc}$  and  $4 \text{ km s}^{-1}$  respectively. These particles are released instantaneously at the pericenter  $8 \text{ kpc}$  from the center  $4 \text{ Gyrs}$  ago. These parameters might be most relevant for satellites such as the progenitor of the Sagittarius stream. We simulate observations of mock data of 100 bright Horizontal Branch stars convolved with GAIA accuracy.

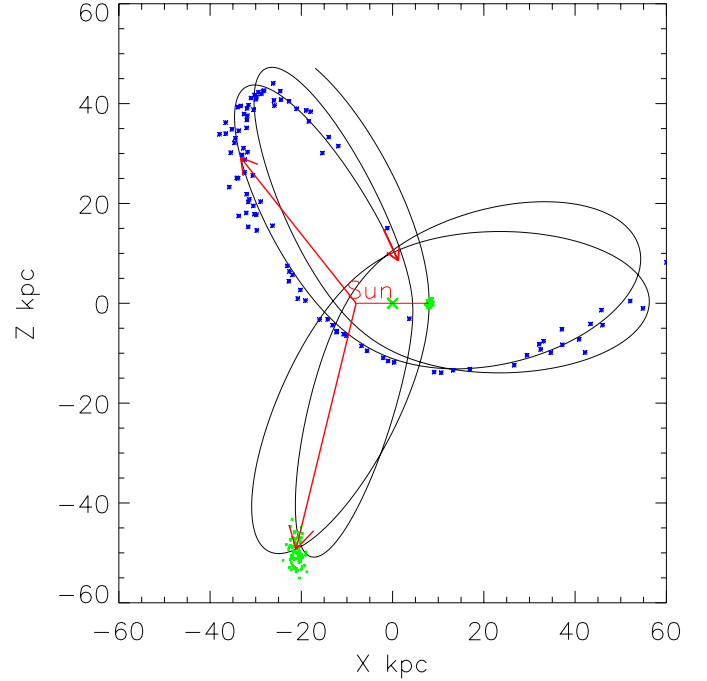


**Fig. 1.** Simulated orbit of the parent satellite and the released stream of about 100 giant stars in a potential model with a growing disc  $\Phi_G$ . The Galactic center is marked by a cross. We assume that the parent satellite is totally disrupted 4 Gyrs ago at a pericenter  $8 \text{ kpc}$  (Sun’s mirror image point) and moving south (down) with a velocity  $380 \text{ km s}^{-1}$ . The stubby debris tail shortly ( $0.3 \text{ Gyrs}$ ) after the disruption is also shown together with the well-developed tidal tail 4 Gyrs later; the center of the satellite circles around like the arms of a clock, with its position at different epoch is indicated by the long arrows.

Johnston (1998) showed that a satellite on rosette orbits in the outer halo  $\geq 20 \text{ kpc}$  leaves behind a nice thin spaghetti-like tail. Helmi & White (1999) put their satellites on plunging orbits which come within the solar circle, and found that they become colder in velocity space, but very mixed in the coordinate space after evolving for a Hubble time. While the cold, linear structures seen in Johnston’s simulations are ideal for studying the potential, these stars at large distance are likely too faint for GAIA except for those high up on the tip of the giant branch.

Our choice of the pericenter of the satellite is somewhere in between previous authors. We concentrate on satellites which fall in and are disrupted recently (about 4 Gyrs ago, well after the violent relaxation phase) and maintain a cold spaghetti-like structure. We put the satellites on relatively tight orbits but which lie outside the solar circle (pericenter of about  $8 \text{ kpc}$  and apocenter of about  $40 \text{ kpc}$ ) such that the bright member stars in the stream are still within the reach of detectability of GAIA. Such streams typically go around the Galaxy less than 5 times since disruption, and are typically far from fully phase-mixed. The morphology of a simulated stream in the potential described in §2.1 is shown in Fig. 1, where the orbit of the disrupted satellite is chosen so that the released stream stays in the polar  $xz$  plane, which passes through the location of the Sun and the Galactic center; the  $xyz$  coordinate is defined such that the Sun is at

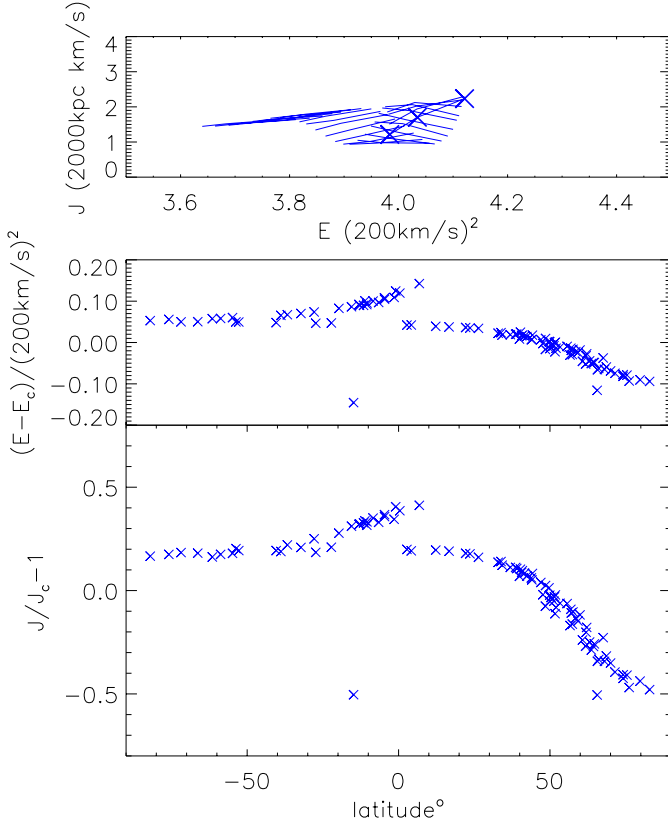


**Fig. 2.** The lower panels show the angular momentum and energy along the stream simulated in the same time-varying potential as in Fig. 1.  $J_c$  and  $E_c$  are the present values for the center of mass of the stream. The top panel shows how most ( $\sim 70\%$ ) stars in a stream evolve in the energy vs. angular momentum plane. Each short line segment is the distribution at an epoch; the present epoch is marked by the crosses. We advance the stream in steps of about 0.15 Gyr from 4 Gyrs ago to present.

$x = -8$  kpc and  $y = z = 0$ . We can see (cf. Fig. 2) that by and large the energy  $E$  of particles across each stream is spread out only in a narrow range at each epoch in the three models; the same holds but to a lesser extent for the angular momentum vector  $\mathbf{J}$ . This implies that stars in the stream are largely coeval even in the presence of realistic, moderate evolution of the Galactic potential. The energy and angular momentum is also modulated with particle position in a sinusoidal way across the stream, an effect which in principle can be used to infer the evolution rate of the Galactic potential and the flattening of the potential.

### 2.3. Some analytical arguments

To understand the above results analytically, let's follow the energy evolution of two particles (1 and 2) in an extremely simplified evolution history of the Galactic potential

$$\Phi(r, \theta, t) = V_0^2 \log r - g|z| \frac{t + t_G}{t_G}, \quad (4)$$

where the potential varies linearly on a time scale  $t_G$  from spherical at time  $t = -t_G$  to a present-day  $t = 0$  flattened potential with a uniform razor thin disk in the  $z = 0$  plane;  $g$  is the surface gravity of the disk. Assume the two particles are released from the satellite with a slight initial energy difference  $\Delta_i$ , which causes them to drift apart in orbital phase. Given enough time the initial phase-bunching of the stream particles should all be dispersed away as a stream can develop tails that wrap around the sky. More generally, we let  $t_{\text{ph}}(\Delta_i)$  be a timescale for the two particles to drift sufficiently apart and become out of phase with each other. The two particles' energy difference ( $E_2 - E_1$ ) at the present epoch  $t = 0$  is then readily computed from

$$E_2 - E_1 = \Delta_i + \int_{-t_G}^0 dt \frac{\partial(\Phi_2 - \Phi_1)}{\partial t} = \Delta_i + \left(\frac{t_{\text{ph}}}{t_G}\right) \xi g z_{\text{max}}, \quad (5)$$

where  $z_{\text{max}}$  is a typical scale height for the orbit, and the dimensionless factor

$$\xi \equiv \frac{1}{t_{\text{ph}}} \int_{-t_G}^0 dt (\eta_1 - \eta_2), \quad 0 \leq \eta \equiv \frac{|z|}{z_{\text{max}}} \leq 1. \quad (6)$$

Interestingly the factor  $\xi$  is of order unity if not smaller. This is because  $\eta_1 - \eta_2$  should take any value between -1 and 1 with equal chance once the two particles are completely out of phase. Hence, we are integrating over an oscillatory function of  $t$  in the range  $-t_G + t_{\text{ph}} \geq t \geq 0$ . This limits  $|\xi|$  at the upper end.

The above equations suggest that: (i) The spread of energy among particles is proportional to the change of the potential, here  $g$  of the disk: particles stay on the same orbit for a static potential. (ii) If the change of the potential is abrupt, e.g., like a step-function, then the energy spread ( $E_2 - E_1$ )  $\sim \Delta_i + g[|z_2| - |z_1|]$  is roughly proportional to the separation of the particles at the time of change. Adjacent particles with  $(z_1 - z_2) \ll z_{\text{max}}$  should also be adjacent in the energy space. This kind of sudden change of potential might be relevant for galaxy formation models with minor infalls on the orbital time scale. (iii) If the potential grows slowly, e.g., adiabatically with  $t_G \rightarrow \infty$ , then we expect only a very small spread in the energy space, no greater than  $|\Delta_i| + \left(\frac{t_{\text{ph}}}{t_G}\right) (g z_{\text{max}})$ . This is consistent with the argument that energy differences between initially similar orbits remain small because of adiabatic invariance of the actions of orbits (as explicitly shown in the spherical case by Lynden-Bell & Lynden-Bell 1995).

### 2.4. Accuracy of parallax and radial velocity from GAIA

Fig. 3 shows the stream in various slices of the 6D phase space observable by GAIA. One of the challenges of using streams to constrain the potential is the measurement errors of proper motion ( $\mu$  in  $\mu\text{as yr}^{-1}$ ), parallax ( $\pi$  in  $\mu\text{as}$ ), and heliocentric radial velocity ( $V_h$  in  $\text{km s}^{-1}$ ), particularly of the latter two. For HB stars, the errors are functions of parallax. We find that this simple formula

$$\text{Err}[\pi] = 1.6 \text{Err}[\mu] = \text{Err}[V_h] = 5 + 50(50/\pi)^{1.5}, \quad (7)$$

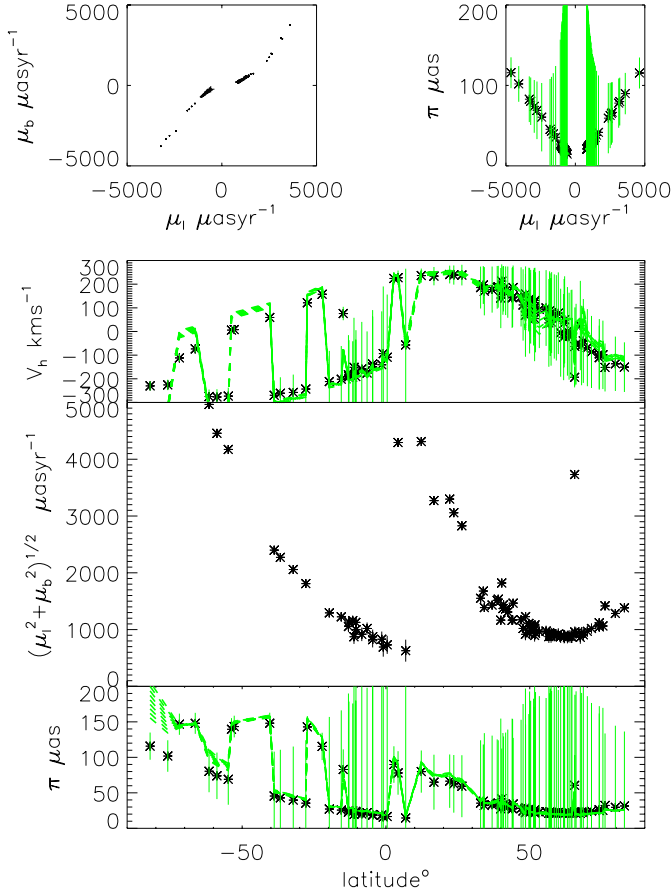


**Fig. 3.** Mock data of the stream convolved with GAIA accuracy for the potential model in Fig. 1. The two small panels at the top are the proper motion vs. proper motion ( $\mu_l$  vs.  $\mu_b$ ) diagram and the (longitude) proper motion vs. parallax ( $\mu_l$  vs.  $\pi$ ) diagram; the linear regression  $|\mu_l| \sim 200 \text{ km s}^{-1}/D \text{ kpc} \sim 40\pi$  manifests the reflex of the Galactic rotation of the Sun and the absence of any azimuthal rotation of a polar stream. The lower three panels show the heliocentric radial velocity, the proper motion, and the parallax across the stream as functions of the latitude, together with their error bars (thin vertical lines); the GAIA error bars for the proper motion are typically much smaller than the size of the symbols. The narrow bands (heavily lines) show parallax and heliocentric velocity predicted from GAIA proper motions, assuming a constant angular momentum  $|\mathbf{J}|$  and approximate energy  $E$  across the stream; the width of the bands here are computed from the initial spread of  $E$  and  $\mathbf{J}$ .

works well in approximating GAIA specifications (Lindgren 1998, private communications) on errors on parallax, proper motion and radial velocity.

Proper motions will be precisely measured everywhere in the Galaxy. A remarkable feature of GAIA is that it can resolve the internal proper motion dispersion of a satellite. Even a small satellite (e.g. a globular cluster) has a dispersion  $\sigma \geq 4 \text{ km s}^{-1}$ . This means that the dispersion in the proper motion is larger than the resolution limit of GAIA for HB stars anywhere within 20kpc ( $\pi \geq 50 \mu\text{as}$ ,  $\text{Err}[\mu] \leq 40 \mu\text{as/yr} = 4 \text{ km s}^{-1}/20\text{kpc}$ , cf. 7). In comparison, radial velocities remain accurate at  $20 \text{ km s}^{-1}$  level, and astrometric parallaxes remain superior

than photometric parallaxes only within 10 kpc ( $\pi \geq 100 \mu\text{as}$ ,  $V \leq 16\text{mag}$ .) because of rapid growth of error bars with magnitude of a star.

Fortunately, a “theoretical” parallax and heliocentric velocity can be predicted to a good accuracy assuming roughly constant angular momentum and energy, i.e.,

$$\mathbf{J} = \mathbf{r} \times \mathbf{V} \sim \text{cst.}, \quad E \sim (200 \text{ km s}^{-1})^2 \log r + \frac{V^2}{2} \sim \text{cst.} \quad (8)$$

Here we pretend that the Galactic potential is the simplest spherical, static and isothermal potential, and feed in the accurately measured proper motions. Surprisingly, these very rough approximations yield fairly accurate parallaxes ( $\sim 10\%$ ) and heliocentric velocities ( $\sim 30 \text{ km s}^{-1}$ ) as shown by the narrow bands in Fig. 3; predictions tend to be poorer for particles in the center and anti-center directions, where the angular momentum  $\mathbf{J}$  becomes insensitive to the heliocentric velocity. But overall it appears promising to apply this method to predict velocities and parallaxes for fainter stars, where the predictions are comparable to or better than directly observable by GAIA. The accuracy of these predictions is verifiable with direct observations brighter members of a stream.

In essence our method is a variation of the classical method of obtaining “secular parallaxes”. A polar stream with zero net azimuthal angular momentum,  $J_z \sim 0$ , makes the simplest example. Any proper motion in the longitude direction  $\mu_l$  is merely due to solar reflex motion, so parallaxes can be recovered to about  $10 \mu\text{as}$  accuracy!) from the linear regression  $\pi \sim |\mu_l|/40$  shown in the top right panel of Fig. 3.

### 2.5. Cool streams

We have run simulations with various parameters for the Galactic potential and orbit and initial size of the satellite. A somewhat surprising result is that streams stay identifiable in a variety of realistic time-dependent potentials. Some examples have been shown in Zhao et al. (1999). As a typical case (cf. Fig. 3) a stream shows up as a narrow feature, clearly traceable in the position-proper motion diagram and the proper motion vs. proper motion diagram after convolving with GAIA errors. The narrowness of the distribution in the proper motion space argues that stars in a stream are distinct from random field stars. While extensive numerical investigations are clearly required to know whether these “cool” linear features can be used to decipher the exact evolution history, evolution itself clearly does not preclude the identification of streams. We caution that the structure of a stream can become very noisy for highly eccentric orbits with a pericenter smaller than 8 kpc and/or for potentials where the temporal fluctuation of the rotation curve is greater than 10%. These noisy structures as a result of strong evolution can be challenging to detect.

We conclude that tidal streams are excellent tracers of the Galactic potential as long as a stream maintains a cool, spaghetti-like structure, in particular, the results of Johnston et al. (1999) and Helmi et al. (1999) for static Galactic potentials are largely generalizable to realistically evolving potentials. However, per-

haps the most exciting implication of these preliminary results is that by mapping the proper motions along the debris with GAIA we could eventually set limits on the rate of evolution of the Galactic potential, and distinguish among scenarios of Galaxy formation.

### 3. Discussions of strategies

#### 3.1. Why targeting streams?

Which is the better tracer of the Galactic potential, stars in a cold stream or random stars in the field? Classical approaches use field stars or random globular clusters or satellites as tracers of the Galactic potential. Assuming that they are random samples of the distribution function (DF) of the halo, one uses, e.g., the Jeans equation, to obtain the potential. One needs a large number of stars to beat down statistical fluctuations, typically a few hundred stars at each radius for ten different radii. The problem is also often under-constrained because of the large number of degrees of freedom in choosing the 6-dimensional DF. Another complication is that one generally cannot make the assumption that the halo field stars are in steady state as an ensemble because it typically takes much longer than a Hubble time to phase-mix completely at radii of 30 kpc or more.

Stars in a stream trace a narrow bunch of orbits in the vicinity of the orbit of the center of the mass, and are correlated in orbital phase: they can all be traced back to a small volume (e.g., near pericenters of the satellite orbit) where they were once bound to the satellite. Hence we expect a tight constraint on parameters of the Galactic potential and the initial condition of the center of the mass of the satellite (about a dozen parameters in total) by fitting the individual proper motions of one hundred or more stars along a stream since the fitting problem is over-constrained.

We propose to select bright horizontal and giant branch stars as tracers of tidal debris of a halo satellite (which we take to be either a dwarf galaxy or a globular cluster). They are bright with  $M_V \leq 0.75$  mag, easily observable  $V \leq 18$  mag within 20 kpc from the Galactic center with GAIA.

#### 3.2. Field contamination

There are numerous HB and GB stars in a satellite. Assume between  $f = 0.5\%$  and  $f = 50\%$  of the stars in the original satellite are freed by two-body relaxation processes (as for a dense globular cluster) and/or by tidal force (as for a fluffy dwarf galaxy). Then the number of HB stars in a stream is

$$N_{\text{stream}} = \frac{f L_V}{(L_V/N_{\text{HB}})} = 10^2 - 10^4, \quad (9)$$

where we adopt one HB star per  $L_V/N_{\text{HB}} = (540 \pm 40)L_\odot$  (Preston et al. 1991) for a globular cluster or a dwarf galaxy with a total luminosity  $L_V = 10^{5-7}L_\odot$ .

In comparison, the entire metal-poor halo has a total luminosity of  $(3 \pm 1) \times 10^7 L_\odot$  and only about  $N_{\text{halo}} = (6 \pm 2) \times 10^4$  HB stars (Kinman 1994). These halo stars are very spread out in velocity with a dispersion  $\sigma_{\text{halo}} \sim 3000 \mu\text{as yr}^{-1}$  in proper motion. So the number of field stars which happen to share the same proper motion with a stream is

$$N_{\text{field}} = N_{\text{halo}} \left( \frac{\sigma_{\text{stream}}}{\sigma_{\text{halo}}} \right)^2 \leq 70, \quad (10)$$

where the dispersion of a stream  $\sigma_{\text{stream}}$  is generously set at  $100 \mu\text{as yr}^{-1}$ , appropriate for a nearby massive dwarf galaxy with velocity dispersion of  $10 \text{ km s}^{-1}$  at 20 kpc. The chance of confusing a HB/GB star in the field with in a stream becomes even smaller if we select stars in a small patch of the sky with similar radial velocities and photometric parallax. In fact Sgr was discovered just on the basis of radial velocity and photometric parallax despite a dense foreground of bulge stars (Ibata, Gilmore, & Irwin 1994). We conclude as far as identifying stars in a cold stream with GAIA is concerned the contamination from field halo stars is likely not a serious problem.

*Acknowledgements.* We thank Amina Helmi for discussions and Tim de Zeeuw and the referee Gerry Gilmore for helpful comments on an earlier draft.

### References

- Gilmore G. et al. 1998, Proc SPIE Conference 3350, March 1998 (in press) Astronomical Interferometry
- Grillmair C.J. et al. 1998, Workshop on Galactic Halos, Santa Cruz, ed. D. Zaritsky (astro-ph/9711223)
- Helmi A. & White S.D.M. 1999, MNRAS, in press
- Helmi A., Zhao H.S., & de Zeeuw P.T. 1999, astro-ph/9811109
- Ibata R., Gilmore G. & Irwin M.J. 1994, Nature, 370, 194
- Ibata R., Wyse R., Gilmore G., & Irwin M. & Suntzeff N. 1997, AJ, 113, 634
- Irwin M. J. & Hatzidimitriou D. 1995, MNRAS, 277, 1354
- Johnston K. 1998, ApJ, 495, 297
- Johnston K.V., Zhao H.S., Spergel D.N., Hernquist L. 1999, ApJ, 512, L109
- Kinman, T.D. 1994, Stellar populations, IAU Symp. 164, P.C. van der Kruit, G. Gilmore (Dordrecht: Kluwer), p75.
- Lynden-Bell D. & Lynden-Bell R.M. 1995, MNRAS, 275, 429
- Ostriker E. & Binney J.J. 1989, MNRAS, 237, 785
- Preston G., Shectman S., Beers T. 1991, ApJ, 375, 121
- Zhao H.S., Johnston K.V., Spergel D.N., Hernquist L., 1999, astro-ph/9901071